

## Attenuation of Swell by Sea Ice

PETER WADHAMS

*Scott Polar Research Institute, University of Cambridge, Cambridge, England*

A mechanism of steady state creep is proposed to describe the attenuation rate of long-period ocean waves in fields of sea ice. It is shown that this mechanism fits the existing wave observations of *Robin* [1963] and *Wadhams* [1973] provided a Glen-type flow law is employed with an exponent  $n = 3$  and a flow law parameter ( $B$ ) similar to the value for polycrystalline ice near the melting point.

Observations of the penetration of ocean waves into sea ice have shown that two extreme types of effect can be distinguished. The short-wave component of a sea is very rapidly attenuated, and within a few hundred meters of the ice edge its energy has largely disappeared [Dean, 1973]. Long-period waves and swell, however, are still detectable several hundred kilometers into the ice [Robin, 1963].

When exposed to an incident wave, each volume element of an ice floe passes through a cycle of alternating tension and compression. The major part of the deformation thus induced is elastic, but it is accompanied by a time dependent plastic strain (creep). The creep process requires work, which involves the absorption of energy from the wave. We hope to show that a creep mechanism provides an adequate description of the observed attenuation rates of long waves in floating ice, and we also will examine how far the results are applicable to sea waves of shorter period.

### RATE OF ENERGY LOSS DUE TO CREEP

We consider a simplified geometry shown in Figure 1. A semi-infinite sheet of ice of constant thickness  $2h$  floats in water of depth  $D$ . A monochromatic wave with a plane wavefront is propagating into the ice at right angles to the ice edge. We assume that no plastic strain can occur in the  $y$  direction. The orthogonal system of axes shown has  $x$  as horizontal, but for stress analysis we assume that  $x$  can always be taken as parallel to the ice surface.

Each element of the ice is subject to a

sinusoidal stress cycle consisting of two 'loading phases' in which the magnitude of the stress is increasing and two 'unloading phases' in which it is decreasing. In the loading phase, forward creep occurs: *Tabata* [1958] found that a constant tensile stress applied to sea ice first produces rapid transient creep, which slows after a few minutes to steady state creep with a constant strain rate. In the absence of laboratory experiments on the behavior of ice under dynamic stresses we cannot be certain if these results still apply. In addition we do not know how much creep occurs during the unloading phase. Therefore we shall test one possible model of the creep process against the observational evidence, and then we shall consider what modifications may be necessary. Our assumption is that steady state creep, obeying the flow law of *Glen* [1955] with a constant flow law exponent, occurs through all phases of the stress cycle.

Each phase lasts less than 5 sec, and in such a time it is found [Tabata, 1958] that the absolute creep strain is two orders of magnitude less than the elastic strain. Thus the creep has little opportunity to relax the stress, so we can make the further assumption that the stress can be derived directly from the degree of bending of the sheet using linear elastic theory.

For an element of ice at  $(x, y, z)$  the flow law as formalized by *Nye* [1953] gives

$$\left(\frac{d\epsilon}{dt}\right)_{ij} = \frac{\tau^{n-1}}{B^n} \sigma_{ij}' \quad (1)$$

where  $\tau$  is the effective shear stress  $|\frac{1}{2}\sigma_{ij}'|$ ,  $\sigma_{ij}'$  is the deviatoric stress tensor  $\sigma_{ij} - p$ ,  $p$  is the hydrostatic pressure,  $(d\epsilon/dt)_{ij}$  is

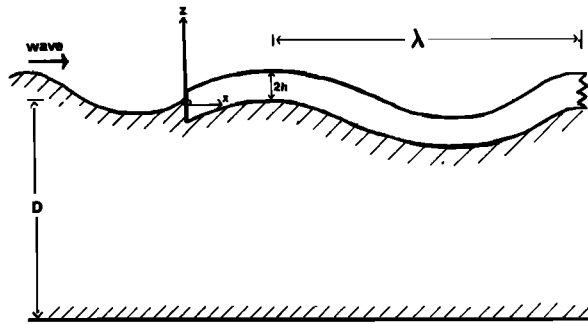


Fig. 1. A wave entering an ice field.

the strain rate tensor,  $i, j$  is 1-3, and  $B$  and  $n$  are flow law parameters,  $n$  being a constant and  $B$  a function of temperature.

Principal stresses are  $\sigma_{11}$ ,  $\sigma_{22}$ , and  $\sigma_{33}$ , and if we neglect shear stresses due to bending we can identify the principal axes as  $x, y$ , and  $z$ , so that

$$\tau^2 = \frac{1}{2}(\sigma_{xx}'^2 + \sigma_{yy}'^2 + \sigma_{zz}'^2) \quad (2)$$

The mean shear stress due to bending (i.e., of the form  $\sigma_{xz}$ ) is a fraction  $4h(1 - \nu^2)/3\lambda$  of the tensile stress averaged over thickness at the wave crest, where  $\nu$  is Poisson's ratio and  $\lambda$  is the wavelength. For  $\lambda = 200$  meters this fraction is only 2% and diminishes for increasing wavelength. We shall also neglect stresses tending to cause the sheet to spread outwards under its own weight [Weertman, 1957], which are less than 1% of tensile stress for  $\lambda = 200$  meters.

We thus have

$$\begin{aligned} \sigma_{xx}' &= \sigma_{xx} - p \\ \sigma_{yy}' &= \sigma_{yy} - p \\ \sigma_{zz}' &= \sigma_{zz} - p \end{aligned} \quad (3)$$

Now  $\sigma_{zz} = 0$  from our elastic bending assumption, and we have assumed that  $\sigma_{yy}' = 0$ . For zero dilatation we must have  $\sigma_{xx}' = -\sigma_{zz}'$ , so equations 3 yield

$$\sigma_{xx}' = \sigma_{zz}/2 = -\sigma_{zz}' \quad (4)$$

and from (2)

$$\tau = |\sigma_{zz}/2| = \sigma_{xx}' \quad (5)$$

We can therefore state the flow law as

$$\left(\frac{d\epsilon}{dt}\right)_{xx} = (\sigma_{xx}/2B)^n \quad (6)$$

Then the rate of energy loss per unit volume within the ice due to creep is

$$\frac{dW}{dt} = \sigma_{,i} \left(\frac{d\epsilon}{dt}\right)_{,i} = \sigma_{zz} \left(\frac{d\epsilon}{dt}\right)_{zz}$$

and in our case

$$\frac{dW}{dt} = |\sigma_{zz}^{n+1}/(2B)^n| \quad (7)$$

Now the profile of flexure of the sheet of ice, and hence the wave, is given by

$$\xi = {}_x A_i \sin 2\pi(x/\lambda - t/T) \quad (8)$$

where  ${}_x A_i$  is the amplitude of flexure of the sheet at a penetration  $x$  and  $T$  is the wave period.

The tensile stress  $\sigma_{xx}$  at the ice surface ( $z = h$ ) is given by the theory of elastic bending as

$$\sigma_{xx}(h) = -\frac{Eh}{(1 - \nu^2)} \frac{\partial^2 \xi}{\partial x^2} = \frac{4\pi^2}{\lambda^2} \xi \frac{Eh}{(1 - \nu^2)} \quad (9)$$

where  $E$  is Young's modulus for the ice. Also, by assuming a linear variation of stress about a neutral axis at the center of the sheet,

$$\sigma_{xx}(z) = (z/h)\sigma_{xx}(h)$$

so from (7),

$$\frac{dW}{dt}(x, z) = 2B \left| \frac{2\pi^2 E \xi z}{B \lambda^2 (1 - \nu^2)} \right|^{n+1} \quad (10)$$

For a unit width of ice field taken perpendicular to the wave vector the rate of energy loss per unit length is

$$\begin{aligned} \frac{dQ}{dt}(x) &= 2 \int_0^h \frac{dW}{dt}(x, z) dz \\ &= 2 \left| \frac{(4\pi^2 E \xi / \lambda^2 (1 - \nu^2))^{n+1} h^{n+2}}{(2\langle B \rangle)^n (n + 2)} \right| \end{aligned} \quad (11)$$

where  $\langle B \rangle$  is the flow law parameter averaged over the depth of the ice.

ATTENUATION OF WAVE AMPLITUDE

We now introduce a factor  $R$  such that (energy/unit surface area of wave in ice sheet) =  $\frac{1}{2} \rho g R {}_x A_i^2$ , where  $\rho$  is the density of sea water.  $R$  is a factor of proportionality designed to make this expression identical with the equivalent expression for a wave in open water.

The average rate of energy transmission in the direction of the wave, per unit width across the wavefront, is then:

$$\begin{aligned} [\text{energy/unit surface area}] \\ \cdot [\text{group velocity of wave}] &= \frac{1}{2} \rho g R {}_x A_i^2 \cdot U \end{aligned} \quad (12)$$

The rate of energy loss between  $x$  and  $x + dx$  is

$$-\frac{1}{2} \rho g UR \cdot 2 {}_x A_i \cdot d {}_x A_i \quad (13)$$

and we equate this to the rate of energy loss due to creep in that distance which from (11) is

$$K \frac{h^{n+2}}{\lambda^{2n+2}} \langle |\xi|^{n+1} \rangle dx \quad (14)$$

where

$$K = 2 \left( \frac{4\pi^2 E}{(1 - \nu^2)} \right)^{n+1} \frac{1}{(2\langle B \rangle)^n (n + 2)}$$

a function of ice properties only, and  $\langle |\xi|^{n+1} \rangle$  is an average taken over one wave period. Now

$$\begin{aligned} \langle |\xi|^{n+1} \rangle &= {}_x A_i^{n+1} \cdot \frac{1}{\pi} \int_0^\pi \sin^{n+1} \beta d\beta \\ &= {}_x A_i^{n+1} I_n \end{aligned}$$

say, with  $I_n = \frac{1}{2}$  for  $n = 1$  and  $< \frac{1}{2}$  for  $n > 1$ .

By equating (13) and (14)

$$\frac{d {}_x A_i}{dx} = -S {}_x A_i^n \quad (15)$$

where

$$S = \frac{K h^{n+2} I_n}{\lambda^{2n+2} \rho g UR}$$

The solution is

$${}_x A_i^{n-1} = \frac{1}{(n-1) S x + 1/{}_0 A_i^{n-1}} \quad (16)$$

except in the special case of  $n = 1$  when

$${}_x A_i = {}_0 A_i \exp(-Sx) \quad (17)$$

Figure 2 shows the general shape of the decay of  ${}_x A_i^2$  (proportional to the wave energy density) with increasing penetration.

Before we can compare this with observational data we need to derive values for  $U$  and  $R$ ; this derivation follows in the next two sections.

*Group velocity of a wave in ice.* The following treatment is based with modifications on an analysis by Greenhill [1887]. The resulting equations were verified by Ewing and Cray [1934] for the case of ice cover on a canal.

Assuming that the water is incompressible and that the flow due to the wave is irrotational, we can define a velocity potential  $\phi$  within the water such that at every point it obeys the equation of continuity (Laplace's equation)

$$\nabla^2 \phi = 0 \quad (18)$$

with the boundary conditions

$$\frac{\partial \phi}{\partial z} = 0 \quad z = -D \quad (19)$$

and

$$\frac{\partial \phi}{\partial z} = -\frac{\partial \xi}{\partial t} \quad z = 0 \quad (20)$$

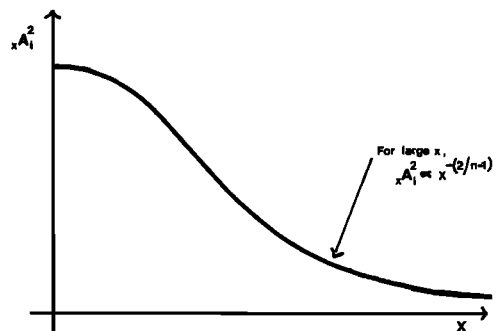


Fig. 2. Schematic diagram of decay of wave energy with penetration.

assuming  $D \gg h$ . A solution to this is

$$\phi = \frac{\omega_x A_i}{k} \frac{\cosh k(z + D)}{\sinh kD} \cos(kx - \omega t) \quad (21)$$

where  $k = 2\pi/\lambda$  and  $\omega = 2\pi/T$ .

If  $\delta p$  is the excess of pressure just beneath the ice-water interface over atmospheric pressure, then by Bernoulli's equation taken to first order,

$$(\delta p/\rho) + g\xi - (\partial\phi/\partial t) = 0 \quad (22)$$

But the equation of motion of the ice is

$$2h\rho_i \frac{\partial^2 \xi}{\partial t^2} = -L \frac{\partial^4 \xi}{\partial x^4} + \delta p \quad (23)$$

where  $\rho_i$  is the density of the ice and  $L$  is the flexural rigidity of ice, equal to  $\frac{2}{3}[h^3 E/(1 - \nu^2)]$ , assuming that the inertia of each section of ice is concentrated at its center.

Equations 21-23 yield

$$c^2 = \frac{\omega^2}{k^2} = \frac{g\rho/k + Lk^3}{\rho \coth kD + 2h\rho_i k} \quad (24)$$

where  $c$  is the phase velocity of the wave within the ice field. For ice fields over continental shelves it may be necessary to use this form, but over an abyssal plain where  $kD \gg 1$  we can approximate  $\coth kD$  to unity, giving

$$c^2 = \frac{g\lambda}{2\pi} \left[ \frac{1 + (2\pi F/g\lambda^4)}{1 + G/\lambda} \right] \quad (25)$$

where

$$F = \frac{16}{3} \frac{\pi^3 h^3 E}{(1 - \nu^2)\rho}$$

$$G = \frac{4\pi h\rho_i}{\rho}$$

The group velocity

$$U = c - \lambda \frac{dc}{d\lambda} = \frac{c}{2} \left[ \frac{1 + (4F/\lambda^3 c^2)}{1 + G/\lambda} \right] \quad (26)$$

For thin ice,  $F$  and  $G$  are small and  $c$  tends toward the familiar value for open water of infinite depth, with  $U$  tending to  $c/2$ .

Figures 3 and 4 summarize how  $c$ ,  $U$ , and  $\lambda$  vary with wave period for different ice thicknesses. The graphs were plotted using the typical values  $E = 6.10^9$  N m<sup>-2</sup> and  $\nu = 0.3$  (best average values for permanent polar ice obtained from *Lavrrov* [1969]),  $\rho_i/\rho = 0.9$ , and  $\rho = 1025$  kg m<sup>-3</sup>. It can be seen that at all except the longest periods  $\lambda$  is greater than its open water value for a given period. For short waves  $U > c$ , and both  $U$  and  $c$  have minimums at midperiod. The behavior is thus greatly unlike that of open water except at the longer periods.

We can draw an important conclusion from these results. For long-period waves the phase velocities in ice and in open water are almost the same, so that a wave does not 'see' the

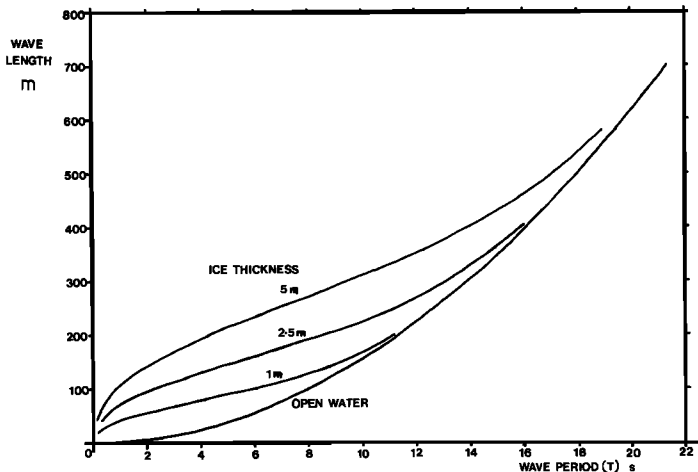


Fig. 3. Variation of wavelength in ice with wave period.

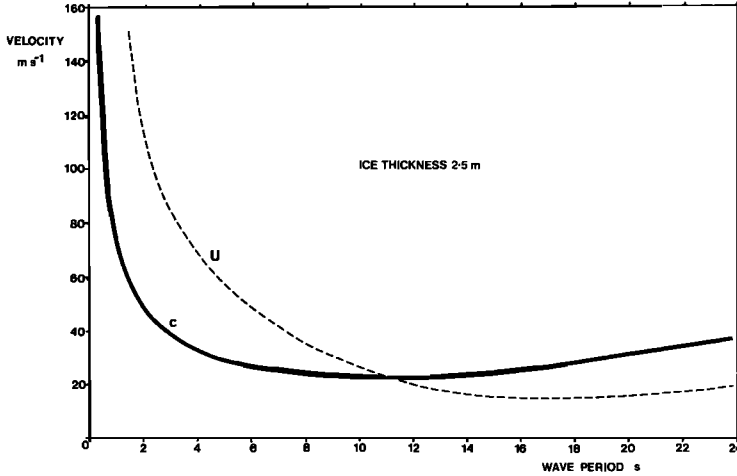


Fig. 4. Dispersion relation for phase and group velocities.

edge of a floe. An ice field in the form of finite floes separated by narrow leads will therefore have virtually the same attenuating effect as a continuous sheet, provided the average floe diameter is at least double the wavelength (otherwise considerable reduction in bending stress occurs). For shorter waves there is an impedance mismatch between ice and water, resulting in multiple scattering and reflection at floe edges. In nature the portion of an ice field which abuts upon the open sea is almost always broken up into finite floes, so we conclude that the simple theory developed here cannot be applied to waves of short period. From Figure 3 the transition to validity occurs at about a 10- to 14-sec wave period for ice 2 meters thick.

*Energy density of a wave in ice.* The propagation of a water wave through ice involves a complex exchange of the kinetic and potential energies of the ice and underlying water, respectively. We shall consider average values of each quantity over a wavelength.

If  $u$  and  $v$  are the  $x$  and  $z$  components of water particle velocity at the point  $(x, y, z)$ , then from (21)

$$u = -\frac{\partial\phi}{\partial x} = \frac{\omega_x A_i \cosh k(z + D)}{\sinh kD}$$

$$\cdot \sin(kx - \omega t) = \omega_x A_i \exp(kz)$$

$$\cdot \sin(kx - \omega t) \quad D \geq \lambda/2 \quad (27)$$

$$v = -\frac{\partial\phi}{\partial z} = -\omega_x A_i \exp(kz) \cdot \cos(kx - \omega t)$$

Then the average kinetic energy of the water per unit area of surface

$$E_1 = \frac{1}{\lambda} \int_{-\infty}^0 \int_0^\lambda \rho \left( \frac{u^2 + v^2}{2} \right) dx dz \quad (28)$$

$$= \frac{\rho \omega_x^2 A_i^2}{4k}$$

The potential energy stored in the water per unit surface area is

$$E_2 = \frac{1}{\lambda} \int_0^\lambda \frac{\rho g \xi^2}{2} dx = \frac{\rho g_x A_i^2}{4} \quad (29)$$

Now each element of the ice cover moves only in the  $z$  direction with velocity  $d\xi/dt$ , so an element of unit width and length  $dx$  has instantaneous kinetic energy  $h dx \rho_i (d\xi/dt)^2$ . Thus the average kinetic energy of the ice per unit surface area is

$$E_3 = \frac{1}{\lambda} h \rho_i \int_0^\lambda \left( \frac{d\xi}{dt} \right)^2 dx = \frac{\omega^2 h \rho_i A_i^2}{2} \quad (30)$$

When a sheet of ice is flexed to a profile  $\xi(x)$  it exerts a vertical stress  $s(\xi)$  on the underlying water of

$$s(\xi) = -\frac{2Eh^3 d^4 \xi}{3(1 - \nu^2) dx^4}$$

Thus the work done per wavelength in establishing this profile is

$$-\int_0^\lambda \int_0^\xi s(\xi) d\xi dx = \frac{Eh^3k^4 \tau A_i^2 \lambda}{6(1-\nu^2)}$$

giving an average potential energy of the ice per unit surface area of

$$E_4 = \frac{Eh^3k^4 \tau A_i^2}{6(1-\nu^2)} \tag{31}$$

By the conservation of energy,

$$E_1 + E_2 + E_3 + E_4 = \frac{1}{2}\rho g R \tau A_i^2 \tag{32}$$

and by applying (26) and (27) we find that

$$E_1 + E_3 = E_2 + E_4 \tag{33}$$

i.e., the average kinetic and potential energies of the combined ice/water system are equal, the result expected for a progressive wave. Then from (32),

$$R = 1 + \frac{32Eh^3\pi^4}{3\rho g\lambda^4(1-\nu^2)} \tag{34}$$

In Figure 5,  $R$  is plotted against wave period for different ice thicknesses.

COMPARISON WITH OBSERVATIONAL DATA

There have been no direct laboratory experiments on the flow law of sea ice. Walker [1970], in experiments on the creep of polycrystalline ice at stresses between 0.1 and  $2 \times 10^6$  N m<sup>-2</sup>, found that his results were

best fitted by a flow law with  $n = 3$ , with no evidence of reversion to Newtonian ( $n = 1$ ) flow at lower stresses. Thomas [1971] showed that the creep of ice shelves involving stresses between 0.04 and  $0.1 \times 10^6$  N m<sup>-2</sup> can also be described by an  $n = 3$  flow law. The maximum stresses involved in wave action given by (9) are of the order  $1 \times 10^6$  N m<sup>-2</sup>. We shall therefore take an  $n = 3$  flow law for sea ice and examine whether this fits observational data.

Equation 16 then becomes

$$\tau A_i^2 = 1/(2Sx + 1/a A_i^2) \tag{35}$$

$aA_i$ , the amplitude of flexure just inside the ice edge, is not a readily measurable quantity, and it is more convenient to choose as a base line the amplitude at a small penetration  $x = a$ , giving

$$(1/x A_i^2) - (1/a A_i^2) = 2S(x - a) \tag{36}$$

The results of Robin. Robin [1963] made measurements from R.R.S. John Biscoe with a shipborne wave recorder during two complete transits of the Antarctic pack ice belt between South Georgia and Halley Bay.

The National Institute of Oceanography wave recorder [Tucker, 1956] with a combination of accelerometers and a pressure transducer records objective wave height in open water. In an ice field, provided the vessel is not held fast, it is reasonable to suppose that

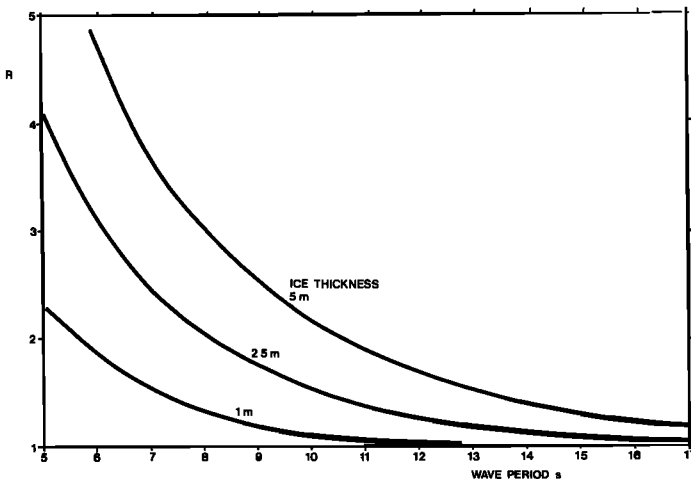


Fig. 5. Variation of  $R$  with wave period for different ice thicknesses.

the recorder measures the objective height of waves in the small pool of open water that the vessel occupies. If we call this height  $x A_w$  and assume continuity of energy when the wave leaves the ice to enter the pool (Figure 6), then from (12)

$$\frac{1}{2} \rho g x A_w^2 \cdot \frac{c_0}{2} = \frac{1}{2} \rho g R x A_i^2 \cdot U \quad (37)$$

provided  $D \geq \lambda/2$ , where  $c_0 = gT/2\pi$  is the phase velocity of the wave in open water. Equation 36 then becomes

$$\frac{1}{x A_w^2} - \frac{1}{a A_w^2} = \frac{Sc_0}{UR} (x - a) \quad (38)$$

The validity of this assumption depends on the size of the pool and the boundary conditions at its periphery: the real wave height probably lies between  $x A_i$  and  $x A_w$ . In the case of long-period waves this is not a serious problem, since  $x A_i$  and  $x A_w$  are almost identical.

Robin calculated the spectral energy density of the 16-sec wave component at different penetrations for the two transits. Figure 7 shows his results replotted in a form compatible with (38). In each case the first measurement made inside the ice was taken as the  $x = a$  datum. The ice field was taken to begin at 66°S for the outward voyage and 67°S for the return, and the ice edge was assumed to run east-west in each case. Robin gives a range of values for ice thickness, but for the outward voyage he indicates a distinct thickening half-way through the transit. Accordingly an attempt was made to fit two straight lines to the data for the outward voyage and a single line for the return.

The scatter in the data points derives from two sources. First, the energies were obtained

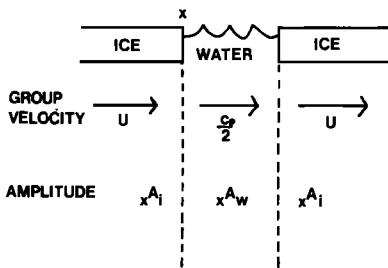


Fig. 6. Effect of a narrow lead at right angles to wave vector.

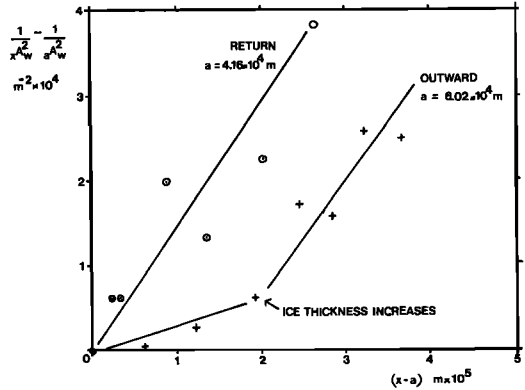


Fig. 7. Plot of  $(1/x A_w^2 - 1/a A_w^2)$  against  $(x - a)$  for the observations of Robin [1963].

by the power spectrum analysis of 10-min wave records, yielding a statistical uncertainty of  $\pm 40\%$  in each energy value. Second, fluctuations in ice thickness cause large changes in the gradient of the graph. Equation 38 predicts the gradient to be

$$\frac{Sc_0}{UR} = \frac{12h^5 T}{5\pi\lambda^8 \rho U^2 R^2 \langle B \rangle^3} \left( \frac{\pi^2 E}{1 - \nu^2} \right)^4 \quad (39)$$

For long-period waves  $\lambda$ ,  $U$  and  $R$  are relatively insensitive to variations in  $h$ , so that for a given wave period the gradient is proportional to  $h^5$ . Taking into account this unavoidable scatter, the fit of the data to a straight line is remarkably good, providing evidence for the validity of an  $n = 3$  flow law.

Robin estimated ice thickness by eye and noted that these were likely to be underestimates. If we take the upper limit of each range of estimates as being a true typical ice thickness we obtain from the lines of best fit

Outward voyage:

Thin ice, 1.6 meters

$$\langle B \rangle = 3.2 \times 10^7 \text{ Nm}^{-2} \text{ sec}^3$$

Thick ice, 2.1 meters

$$\langle B \rangle = 3.1 \times 10^7 \text{ Nm}^{-2} \text{ sec}^3$$

Return voyage, 1.6 meters:

$$\langle B \rangle = 2.0 \times 10^7 \text{ Nm}^{-2} \text{ sec}^3$$

To gage the reliability of these values of  $\langle B \rangle$  we must consider both the limitations of

our model and the possibility of other physical processes occurring. Our model has employed three simplifying assumptions: constancy of ice thickness, a continuous sheet of ice, and a wave vector that runs perpendicular to the edge. We have shown that variations in ice thickness have a very large effect, so that features such as bergy bits and very thick old floes, although occupying only a small fraction of the ice field, will cause a disproportionately high loss of wave energy. For long waves the effect of finite-sized floes is small, since the reflection coefficient is offset by the reduction in the rate of energy loss due to the partial coverage of the surface. The effect of a wave entering the ice at a slant is greater. If the wavefront is at an angle  $\theta$  to the ice edge the wave vector travels a distance

$$d = x \sec \theta \quad (40)$$

to achieve a penetration  $\hat{x}$ . By starting from a datum line inside the ice we ensure that waves with  $\theta$  close to  $\pi/2$  will never enter the field of measurement in the first place, but a value as high as  $\pi/3$  is conceivable.  $\langle B \rangle \propto (d/x)^{2/3}$ , a factor which is 1.26 for  $\theta = \pi/3$ . A wave recorder measurement tells us nothing about the directional spectrum, so we must conclude on the basis of this and the other two effects that  $\langle B \rangle$  may be greater than the derived value by up to 50%.

The possibility of other physical processes arises from the large distances (at least 400 km) involved in Robin's measurements. A swell can gain energy directly by the pressure of a following wind, and energy can be added indirectly by the effect of air pressure fluctuations passing over the ice sheet [Sytinskii and Tripol'nikov, 1964]. Phillips [1969] has shown that weak coupling between the swell and an adverse wind and the breaking of locally generated short waves as they ride over the crests of a swell are the two significant mechanisms that can cause a swell to lose energy. Finally, we have tacitly assumed that the energy spectrum of the open sea near the ice edge has remained constant while the wave recordings were taken. The 16-sec wave component normally originates from a distant storm, and so its energy density is likely to vary considerably over a period of hours.

These mechanisms add to the uncertainty in our results, and our best estimate of  $\langle B \rangle$  is  $(3 \pm 2) \times 10^7 \text{ N m}^{-2} \text{ sec}^3$ . Figure 8, taken from Thomas [1971], shows Walker's laboratory curve of the variation of  $\langle B \rangle$  with temperature in pure polycrystalline ice. Our value of  $\langle B \rangle$  for sea ice is close to the value for polycrystalline ice at the melting point. Only near the melting point does polycrystalline ice have significant aqueous intrusions along grain boundaries, whereas sea ice has brine inclusions at all temperatures [Lewis, 1971]. Thus sea ice over a range of temperatures is likely to have a creep behavior similar to that possessed by polycrystalline ice at the melting point, a conclusion supported by our result.

*The effect of ice thickness.* Robin also plotted for waves of period 16 sec the ratio (energy in ice/open ocean energy) against ice thickness as estimated by eye. The distance of penetration is not given but can be assumed to be large ( $x \gg a$ ) and effectively constant. We also confine ourselves to those data points where the energy ratio is large ( $>10$ ). Under these circumstances we expect that (open ocean energy/energy in ice)  $\propto h^5$ .

Figure 9 is a graph plotted after Robin of  $\log_{10}$  (energy in ice/open ocean energy) against

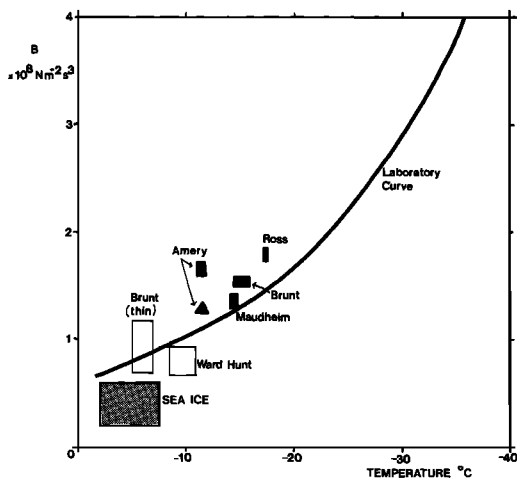


Fig. 8. Plot of flow law parameter  $B$  against temperature, showing Walker's [1970] laboratory results, Thomas's [1971] results for Antarctic ice shelves, more recent data for thin ice shelves (Thomas [1972], open rectangles), and the results of wave observations in sea ice.

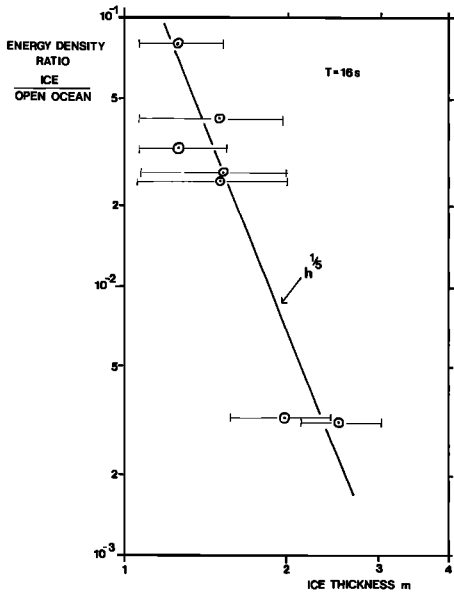


Fig. 9. Log-log plot of (wave energy in ice/wave energy in open ocean) against ice thickness for 16-sec wave component (after Robin [1963]).

$\log_{10} h$ . A straight line of gradient  $-5$  has been drawn through the points and appears to fit the data well, considering the inherent inaccuracy in visual determinations of ice thickness.

*The results of Dean.* Dean [1973], using the same instrument as Robin, made a series of measurements in the Antarctic concentrated near the ice edge, at penetrations of up to 2 km only. For such small penetrations the decay of the long-period components cannot be distinguished against the statistical variance in the spectra. Only the short-period waves decay significantly, and Figure 10 shows plots of  $(1/x A_w^2 - 1/50 A_w^2)$  against  $(x - 50)$  for three values of wave period. Applying (38) to the lines of best fit we obtain the following estimates for  $\langle B \rangle$ :

- $T = 6 \text{ sec} \quad \langle B \rangle = 7.9 \times 10^5 \text{ N m}^{-2} \text{ sec}^3$
- $T = 8 \text{ sec} \quad \langle B \rangle = 4.8 \times 10^6 \text{ N m}^{-2} \text{ sec}^3$
- $T = 9.6 \text{ sec} \quad \langle B \rangle = 8.0 \times 10^6 \text{ N m}^{-2} \text{ sec}^3$

As expected, the values are far too low, showing that the creep model can account for only a small fraction of the energy loss at low periods. Multiple scattering and reflection increase the path length of a wave vector many-

fold, enabling turbulent and viscous losses to become the dominant factors in wave attenuation. A more far-reaching description is needed, and the results will no doubt depend critically on the floe diameter. However, we note that the above estimates of  $\langle B \rangle$  increase with  $T$ , indicating that the creep mechanism begins to take over for  $T > 10 \text{ sec}$ .

*The results of Wadhams.* Wadhams [1973] made a series of wave recordings to the northwest of Spitsbergen with an upward-looking echo sounder mounted on a submerged submarine. The submarine drifted very slowly into the ice so that each record was effectively a time series at a fixed location. Again we must decide whether  $z A_i$  or  $z A_w$  was the parameter being measured. Beneath open water a single echo was received, while below an ice floe a double echo was obtained, consisting of returns from the bottom and top of the floe, respectively. The open water trace, which was continuous with the second return under a floe, was digitized for analysis. Such a trace is thus composed mainly of  $z A_i$ , with an indeterminate admixture of  $z A_w$ .

The power spectra at different penetrations each had a peak at the 12-sec period, and Figure 11 shows  $(1/z A_i^2 - 1/1300 A_i^2)$  plotted against  $(x - 1300)$ , assuming that  $z A_i$  is the measured parameter. The first spectrum, taken at a 1300-meter penetration, was used as the base datum.

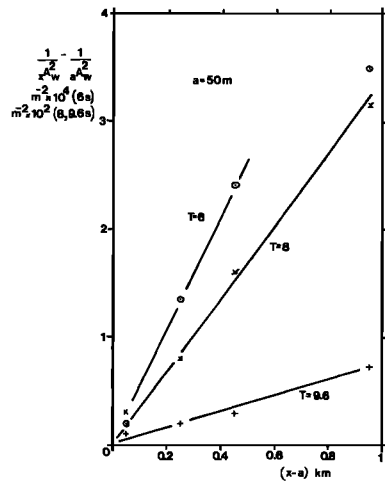


Fig. 10. Plot of  $(1/z A_w^2 - 1/a A_w^2)$  against  $(x - a)$  for the observations of Dean [1972].

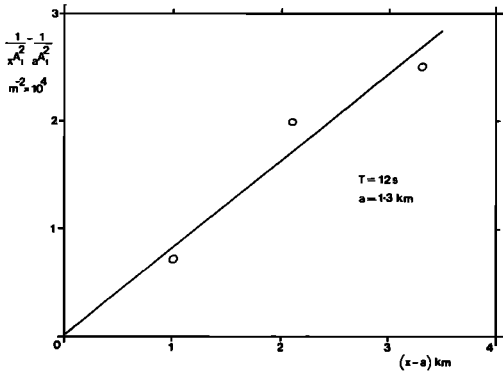


Fig. 11. Plot of  $(1/_{x}A_i^2 - 1/_{a}A_i^2)$  against  $(x - a)$  for the observations of Wadhams [1972].

It can be seen that the points lie close to a straight line. Applying (36) and (38) to the line of best fit yields the estimates for  $\langle B \rangle$ , depending on the assumptions and parameters used, as shown in Table 1.

The ice thickness was estimated visually during surfacings at between 2 and  $2\frac{1}{2}$  meters. The larger value of  $E$  has been considered because Lavrov [1969] in reviewing existing data concludes that perennial Arctic ice tends to be harder than Antarctic ice. However, if we consider the whole thickness of an ice floe including the very soft underpart, we conclude that a lower value of  $E$  is likely to give a better approximation to its behavior. By using the lower of the two values and making additional allowance for the sources of error described earlier, we obtain a best estimate of  $(4 \pm 2) \times 10^7 \text{ N m}^{-2} \text{ sec}^6$  for  $\langle B \rangle$ . This is in good agreement with the value derived from Robin's results.

*Direct measurement of ice flexure.* The ambiguity between  $_{x}A_i$  and  $_{x}A_w$  can be removed by direct measurement of the motion of the ice surface when the parameter in question is simply  $_{x}A_i$ . This offers the best means of obtaining more accurate data with which to test

this model, especially as a suitable array of devices can be used to derive the direction and phase velocity of the waves in ice. Several trials of such a method have been made, of which the best is that of Hunkins [1962], who recorded the deflections of a seismometer and gravity meter in the Beaufort Sea. No numerical conclusions can be drawn from his spectra however on account of the short record length (5 min) and long sampling interval (3 sec). Further observations would be valuable.

*The flow law exponent n.* We have shown that the data of Robin and Wadhams give a straight line when plotted according to (38), furnishing evidence for an  $n = 3$  flow law. If  $n \neq 3$ , (16) cannot be cast into the form of (38), but provided  $_{x}A_i \ll _{a}A_i$  we have approximately

$$1/_{x}A_i^2 = [(n - 1)S(x - a)]^{2/n-1} \quad (41)$$

Despite the scatter in the data it is clear that a value of  $n$  as low as 2, for example, is inadmissible, and we can conclude that  $n$  must lie within the range  $2.5 < n < 3.5$ . This corresponds with laboratory results for various forms of fresh water ice [Weertman, 1972].

The result can be shown more clearly by returning to (15). The differential  $d_{x}A_i/dx$  is estimated from the gradients of smoothed graphs of wave amplitude versus penetration (this was not possible for Robin's return voyage on account of the scatter). A graph is then plotted of  $\log_{10} (d_{x}A_i/dx)$  against  $\log_{10} (_{x}A_i)$  when we expect a straight line of gradient  $n$ .

Figure 12 shows the results. In general,  $n = 3$  fits the data well, except for the outermost points of Robin's observations. Even here we cannot be sure that the  $n = 3$  law breaks down, since these points correspond to a region of the ice field described by Robin as being composed mainly of small floes. If the floe diameter is less than a wavelength, the bending

TABLE 1. Estimates of Flow Law Parameter  $\langle B \rangle$  Using Different Values for  $E$  and  $h$

Measured Quantity	$E = 6 \times 10^9 \text{ N m}^{-2}$		$E = 8 \times 10^9 \text{ N m}^{-2}$	
	$2h = 2 \text{ meters}$	$2h = 2\frac{1}{2} \text{ meters}$	$2h = 2 \text{ meters}$	$2h = 2\frac{1}{2} \text{ meters}$
$_{x}A_i$	$4.3 \times 10^7$	$4.5 \times 10^7$	$2.7 \times 10^7$	$2.9 \times 10^7$
$_{x}A_i^2$	$3.4 \times 10^7$	$3.2 \times 10^7$	$2.1 \times 10^7$	$2.2 \times 10^7$

stress caused by a wave of given amplitude is considerably reduced, thus reducing the rate of energy loss. We should not try to apply our model therefore to fields of small ice floes.

#### DISCUSSION

We find that the observed attenuation rates of waves in ice are fitted best by a Glen-type flow law with an exponent  $n = 3$  and a parameter ( $B$ ) similar to the laboratory value for polycrystalline ice. The range of average tensile stress involved is  $0.1\text{--}0.8 \times 10^6 \text{ N m}^{-2}$  (Robin's results) and  $0.7\text{--}1.3 \times 10^6 \text{ N m}^{-2}$  (Wadhams' results). We must now consider whether this agreement is fortuitous or whether it actually confirms our simple model. In the absence of dynamic stress experiments on ice we must argue by analogy with metal behavior.

A typical effect of stress cycling in metals is to shorten the primary creep stage and bring on steady state creep more quickly. However, since each phase of the cycle due to sea waves lasts for only  $T/4$  (i.e., 5 sec or less), it is unlikely that secondary creep has a chance to establish itself. Therefore in the loading phase the energy loss is more nearly determined by the initial creep rate  $(d\epsilon/dt)_i$ , which is faster than the steady state creep rate  $(d\epsilon/dt)_s$ . Garofalo *et al.* [1963] found for stainless steel a relationship of proportionality between  $(d\epsilon/dt)_i$  and  $(d\epsilon/dt)_s$ , given by

$$\left(\frac{d\epsilon}{dt}\right)_i = 3.3 \left(\frac{d\epsilon}{dt}\right)_s \quad (42)$$

The constant is independent of stress over a wide range and of temperature over the more limited range of the experiment. The data of Chalmers [1937] for tin also show this relationship, with a constant ranging from 3 for large-grained structures to 10 for small-grained polycrystals (sea ice is large-grained). If such a relation is true for ice, then the energy loss will be seen as consistent with the steady state flow law as far as  $n$  is concerned, although ( $B$ ) will be different.

If we now look at the unloading phase, however, we find that experiments such as those of Thompson *et al.* [1955] on aluminum single crystals show that little or no creep occurs. These results are in agreement with Glen [1953], who found that the creep rate of ice

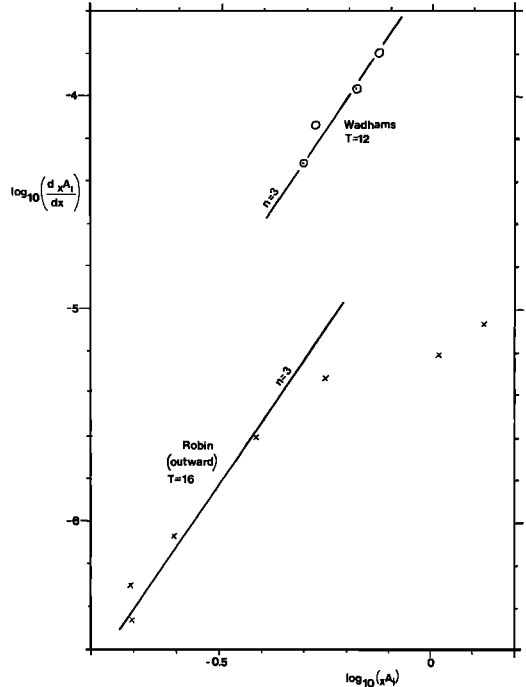


Fig. 12. Log-log plot of rate of amplitude decay against instantaneous amplitude, showing the fit to an  $n = 3$  flow law.

is greatly reduced immediately following a single small reduction in stress.

If no creep occurs during the unloading phase and if in the loading phase we let the ratio  $(d\epsilon/dt)_i/(d\epsilon/dt)_s$  be a constant  $f$ , then the total behavior of the ice over a cycle will mimic a steady state flow law with  $n = 3$  and ( $B$ ) equal to the derived value multiplied by a factor of  $(f/2)^{1/3}$ . This factor will be close to unity if  $f$  is of the same order as that for metals, as is suggested by the creep curves of Tabata [1958]. It is seen therefore that the basic mechanics of our model still hold good and that adjustments to take account of the possible anomalies of cyclic creep involve only slight numerical modifications. Experimental confirmation is required, but it is probable that a creep model similar to that described provides a valid explanation for the attenuation of swell by sea ice.

*Acknowledgments.* I am deeply indebted to R. H. Thomas, who helped to formulate the creep equations, and to Dr. G. de Q. Robin for valuable discussions.

This work was carried out while the author was in receipt of a research studentship from the Natural Environment Research Council of Great Britain.

## REFERENCES

- Chalmers, B., Precision extensometer measurements on tin, *J. Inst. Metals*, *61*, 103-118, 1937.
- Dean, C. H., The attenuation of ocean waves near the open ocean/pack ice boundary, paper presented at Symposium on Antarctic Oceanography, Sci. Comm. on Antarctic Res., Santiago, Chile, Sept. 13-16, 1966.
- Ewing, M., and A. P. Crary, Propagation of elastic waves in ice, *2*, *Physics*, *5*, 181-184, 1934.
- Garofalo, F., C. Richmond, W. F. Domis, and F. von Gemmingen, Strain-time, rate-stress, and rate-temperature relations during large deformations in creep, *Joint Int. Conf. on Creep*, *1*, 31-39, 1963.
- Glen, J. W., Mechanical properties of ice and their relation to glacier flow, Ph.D. dissertation, Univ. of Cambridge, England, 1953.
- Glen, J. W., The creep of polycrystalline ice, *Proc. Roy. Soc. London, Ser. A*, *228*(1175), 519-538, 1955.
- Greenhill, A. G., Wave motion in hydrodynamics, *Amer. J. Math.*, *9*, 62-112, 1887.
- Hunkins, K., Waves on the Arctic Ocean, *J. Geophys. Res.*, *67*(6), 2477-2489, 1962.
- Lavrov, V. V., *Deformation and Strength of Ice*, Gidrometeorologicheskoe Izdatel'stvo, Leningrad, 1969. (Engl. transl. by Israel Prog. for Sci. Trans., Jerusalem.)
- Lewis, E. L., Introduction to Arctic sea ice, *Eng. J., Can. Soc. Civ. Eng.*, *54*, 10-14, 1971.
- Nye, J. F., The flow law of ice from measurements in glacier tunnels, laboratory experiments, and the Jungfraufirn borehole experiment, *Proc. Roy. Soc. London, Ser. A*, *219*(1139), 477-489, 1953.
- Phillips, O. M., *The Dynamics of the Upper Ocean*, pp. 145-154, Cambridge Univ. Press, England, 1969.
- Robin, G. de Q., Wave propagation through fields of pack ice, *Phil. Trans. Roy. Soc. London, Ser. A*, *255*(1057), 313-339, 1963.
- Sytinskii, A. D., and V. P. Tripol'nikov, Some results of investigations of the natural vibrations of ice fields of the central Arctic, *Bull. Acad. Sci. USSR, Geophys. Ser.*, *4*, 370-374, 1964.
- Tabata, T., Studies on visco-elastic properties of sea ice, in *Arctic Sea Ice*, Arctic Sea Ice Conference, Easton, Maryland, 1958.
- Thomas, R. H., Flow law for Antarctic ice shelves, *Nature, London*, *232*(30), 85-87, 1971.
- Thomas, R. H., The dynamics of ice shelves, Ph.D. dissertation, Univ. of Cambridge, England, 1972.
- Thompson, N., C. K. Coogan, and J. G. Rider, Experiments on aluminium crystals subjected to slowly-alternating stresses, *J. Inst. Metals*, *84*, 73-80, 1955.
- Tucker, M. J., A shipborne wave recorder, *Trans. Inst. Nav. Architect.*, *98*, 236-259, 1956.
- Wadhams, P., Measurement of wave attenuation in pack ice by inverted echo sounding, paper presented at International Sea Ice Conference, Nat. Res. Council of Iceland, Reykjavik, May 10-13, 1971.
- Walker, J. C. F., The mechanical properties of ice at high homologous temperatures, Ph.D. dissertation, Univ. of Cambridge, England, 1970.
- Weertman, J., Deformation of floating ice shelves, *J. Glaciol.*, *3*, 38-42, 1957.
- Weertman, J., Creep of ice, paper presented at Conference on Physics and Chemistry of Ice, Nat. Res. Council of Canada, Ottawa, August 14-18, 1972.

(Received October 4, 1972;  
revised January 8, 1973.)